Journal of Mechanics in Medicine and Biology
Vol. 12, No. 1 (2012) 1250015 (29 pages)

DOI: 10.1142/S0219519412004454

A QUASI-LINEAR VISCOELASTIC MODEL FOR THE PASSIVE PROPERTIES OF THE HUMAN HIP JOINT

HENDRIK HEGER* and VEIT WANK†

Institute of Sports Science, Eberhard Karls University
Wilhelmstr. 124, Tuebingen, 72074, Germany
**hendrik.heger@uni-tuebingen.de*
†*veit.wank@uni-tuebingen.de*

REINHARD BLICKHAN

Institute of Motion Science, Friedrich Schiller University
Seidelstr. 20, Jena, 07749, Germany
reinhard.blickhan@uni-jena.de

Received 10 January 2011
Revised 20 April 2011
Accepted 5 May 2011

Properties of passive elastic structures constituting the human hip joint can be exploited to increase efficiency of human locomotion. As studies estimating the passive contributions to the net joint moment often disregard damping properties of the joint such contributions overestimate the energy gained during leg retraction within swing and stance phase. We built an experimental apparatus to measure moment-angle-relations during motor guided cyclic movements over a wide range of angular velocities and step-like changes in hip angle. On the basis of the experimentally gained data set the objective of this study was to model the elastic as well as the damping characteristics of the joint in the sagittal plane utilizing the Quasi-Linear Viscoelastic theory (QLV). A double exponential function was conveniently employed to describe the elastic response. The dependency of the hip joint stiffness on biarticular muscles was incorporated by repeating the measurement protocol for different knee angles. Due to the fact that the stiffness characteristics of the elastic response were merely shifted over knee angles we introduced an equilibrium angle at the hip joint as exponential function of the knee angle eventually yielding an elastic response as a function of hip and knee angle. In order to cover the damping characteristics the reduced relaxation function comprising a continuous spectrum of relaxation was utilized. We exemplify the applicability of the QLV model on published kinematic data on human walking and estimated that approximately 27% of the energy passively stored at the hip dissipates during the gait cycle.

Keywords: Biomechanics; passive joint moment; viscoelastic model; QLV theory; human hip joint.

*Corresponding author.

1. Introduction

Passive elastic properties of joints are considered to play an important role in legged locomotion. Their ability to continuously store and release energy during cyclic movement can be exploited to increase movement efficiency.[1,2] In particular the human hip joint with its "soft" boundaries set by the muscles, ligaments and joint capsule seems capable to regain elastic energy from late stance to early swing phase.[3] Net joint moments during walking and running, necessary to generate the movement, are usually determined by inverse dynamics calculations.[4,5] To estimate the passive elastic contribution to net joint moments several methods have been applied to quantify passive moment-angle relations at human joints based on imposed cyclic and step-like movements at the hip,[6,7] at the knee,[8−10] at the ankle,[11−13] and at several leg joints at once.[14−16]

The probably simplest approach to model experimental data acquired during externally guided movement of joints is to derive a nonlinear elastic moment-angle-relation approximately matching the passive properties of the joint and thereby ignore damping.[14,16,17] This is sometimes justified by the assumption that damping effects can be neglected by choosing a quasi-static, i.e., very low, joint angular velocity during measurements. But this assumption is questioned by the facts that even quasi-static conditions normally reveal a considerable hysteresis[6] and that stress relaxation in tendons and ligaments was observed for very long periods of time.[18,19] In addition, the contribution of passive joint properties on the exerted moments and the stored energy during locomotion will likely be overestimated when applying a pure elastic model.[3,16] A simple extension of an elastic approach taking damping into account is to fit the hysteresis loops by two separate functions depending on the direction of movement which is *a priori* limited, for the results are explicitly bound to the measured range of motion.[6]

Hence, for a more accurate estimation, damping effects have to be considered within the modeling approach. One adequate candidate among models of nonlinear viscoelasticity[20] is the quasi-linear viscoelastic theory.[18,21] QLV-models had frequently been used in tissue mechanics and engineering to describe force-length relations[22−26] and stress−strain relations,[27−35] but have not yet been applied to model moment-angle-relations on a macroscopic level, i.e., on the joint level. As joints are formed by tissues that were modeled successfully the same theoretical framework can likely be employed to describe entire joints as well. We therefore utilized the QLV-theory to model the passive viscoelastic properties of the human hip joint.

To acquire a suitable data basis we recorded joint moments for a set of cyclic and step-like angular hip deflections in the sagittal plane. In order to identify the time constants of the reduced relaxation function within the QLV-theory it is necessary that the imposed movements produce responses in a frequency range relevant for the application (e.g., locomotion). However, the frequency window is limited technically (see below) but even more by human factors which are the time of measurement and

the bearable accelerations. Hence, the experimental protocol was designed to weigh practical restrictions with a judicious selection of velocity conditions.

Passive properties of a joint depend on adjacent joints if the joints are coupled by biarticular muscles. Specifically, for the hip joint, biarticular muscles spanning the knee joint have a significant influence on the elastic properties.[6,7,14–16] Hence, the knee angle was taken into account as discrete variable by fixing the knee joint at several constant angles and repeating the measurements at the hip joint for each knee angle consecutively.

In studies conducted on tissue samples the actuated masses are normally small and hence effects of inertia can be neglected. While investigating joints the moment of inertia of the adjacent limb has a considerable impact on the recorded signal. When limbs were moved manually effects of inertia where either diminished by recording at slow speeds[6,14] or their effect was calculated using an inverse dynamics approach.[16] Driving the leg by a motor as has been employed in our study allows for a more precise control of the joint angle and especially acceleration phases. Amankwah *et al.*[15] and Vrahas *et al.*[7] dealt with inertial contributions by blanking out time segments where the leg was accelerated. In our study we assessed the mechanical properties of the experimental apparatus in conjunction with leg inertia by a linear transfer function to separate the moment generated by passive viscoelastic properties from the recorded moment. Thus, continuous moment time courses were available for parameter evaluation.

The objective of this study was to record the joint moments at the hip for a set of cyclic and step-like angle-time-courses to provide a data basis to model the viscoelastic properties of the hip joint. The quasi-viscoelastic theory was utilized to model the passive moment-angle-relationships capturing hysteresis and relaxation processes. The results will be discussed with its application to estimate the contribution of passive joint moments in human locomotion.

2. Materials and Methods

2.1. *Subjects*

All thirteen male volunteer subjects were students or faculty at the Department of Sports Science at the University of Jena, Germany, and athletically active (mean age: 25.4 ± 4.4 years, mean height: 1.80 ± 0.05 m, and mean weight: 78 ± 10.8 kg). None of them reported any traumatic or chronic musculoskeletal disease specifically not at the hip and the knee joint of the left leg. Prior to the experiment the subjects were informed about the purpose of the study and signed the consent form approved by the Ethic commission of the University of Jena.

Subjects included in the study had an individual passive range of motion that was close to or slightly above the boundaries reported in the literature (for typical ranges see Table 1). This resulted in the exclusion of three subjects. None of the subjects were active in sports that require an exceptionally high flexibility at the hip joint, such as in gymnastics.

Table 1. Survey of studies that measured the boundaries for the passive hip joint range of motion.

Authors	Hip extension (degree)	(Knee angle)	Hip flexion (degree)	(Knee angle)
Aalto *et al.*[36]	≈10	(flexed)	100	(0)
Boone and Azen[37]	12	(*)	121	(*)
Greene and Heckman[38]	28	(*)	113	(*)
Kendall and McCreary[39]	10	(0)	120/80	(flexed/0)
Roaas and Andersson[40]	10	(*)	120	(*)
Roach and Miles[41]	19	(*)	121	(*)
Svenningsen *et al.*[42]	23	(*)	37	(*)

Note:*: Measurements were taken with the knee joint placed at an angle according to the procedures described in Greene and Heckman.[38] Flexed: no angular position reported. Angle in degree: Knee angle during measurement of hip joint range of motion.

2.2. *Test apparatus*

2.2.1. *Experimental setup*

An experimental apparatus was constructed which allowed to rotate the human leg through a defined hip range of motion (ROM) at given rates while measuring the exerted moment about the medio-lateral axis of the joint (Fig. 1).

Subjects lay on a padded table in a lateral position. The left leg was strapped to an aluminum lever arm which consisted of two segments connected by a hinge joint. The lever arm was driven by an AC servo-motor (model SK69K, digital servo-controller, model SCE906, Eduard Bautz GmbH, Weiterstadt, Germany) mounted on a height-adjustable rack with the drive shaft vertical. The horizontal position of the table could be adjusted with respect to the drive shaft. A rod could be attached to the drive shaft allowing to manually move the lever arm on demand.

An optical encoder (2000 segments per revolution, Carl Zeiss AG, Jena, Germany) connected to the drive shaft measured the angular velocity. The two encoder channels were wired to quadruple the resolution. Additionally, the motor included a gear with a 12:1 transmission ratio resulting in a resolution of 0.00375 degree per encoder segment. The initial angular position of the leg was determined by a protractor on the rack. The reference angle for the hip joint (0°) was defined as the position where the longitudinal axis of the thigh was aligned with the longitudinal axis of the trunk. The moment was recorded at the drive shaft by a strain gauge transducer (TB1A/500 Nm, amplifier: ME10, HBM, Darmstadt, Germany; used sensitivity: 61.276 Nm/V or 0.1496 Nm per bit; A/D converter with a counter: PCL-711, Advantech Co., US; sampling rate: 1000 Hz).

The lever arm was coupled to the drive shaft by an electromechanical clutch. Subjects could release the clutch via a push button at any time. In addition, electromechanical switches, marking the limits of the subject's range of motion, were attached to the protractor to release the clutch if in contact with the lever arm.

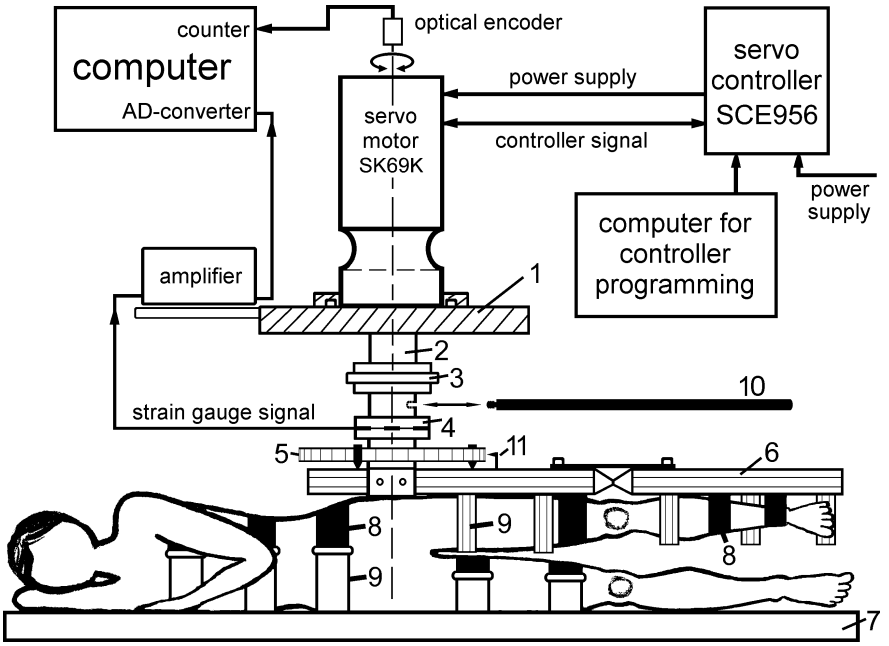

Fig. 1. Schematic of the apparatus: rack (1), drive shaft (2), electromechanical clutch (3), torque measurement device (4), protractor attached to the rack with electromechanical switches (5), aluminum lever arm (6), horizontally adjustable table (7), straps (8), braces (9), rod for manual control (10), pointer on the lever arm to indicate the hip joint position at the protractor.

Surface electromyographic (EMG) signals from three muscles (*M. rectus femoris*, *M. biceps femoris caput longum*, and *M. semitendinosus*) were recorded per subject to examine whether stretched muscles showed reflex activity within the range of motion. Due to severe electromagnetic noise generated by the servo motor EMG was recorded during manual deflection at rates matching those given by the motor. EMG electrodes (Blue Sensor NF, Ambu, Denmark) were positioned in a bipolar configuration according to Delagi *et al.*[43] with the reference electrode placed above the patella. EMG signals were amplified (gain factor 1000) by a Biovision EMG system (Wehrheim, Germany).

2.2.2. *Mechanical properties of the test apparatus*

While moments based on gravitational force were avoided *a priori*, moments of inertia of leg and lever arm contributed significantly to the recorded total moment. Acceleration of the leg induced a slight deflection of the lever arm. The servo in its attempt to reposition the lever behaves like a rotational spring. Thus the response can be described by a second-order transfer function $H(s)$:

$$H(s) = \frac{M(s)}{\alpha(s)} = \frac{J}{a_2 s^2 + a_1 s + 1}. \quad (1)$$

$M(s)$, $\alpha(s)$: Laplace transformed recorded moment and given angular acceleration; J: total moment of inertia of leg and lever arm; a_1, a_2: parameters, $a_1 = \frac{b}{k}$ and $a_2 = \frac{J}{k}$ with stiffness k and damping b; s: Laplace variable.

A representative moment of inertia of 3.6 kgm^2 for a straight leg was calculated from segment lengths and circumferences of thigh, shank and foot of a subject (height: 1.9 m, body weight: 85 kg) using the landmarks and applying the nonlinear regression equations proposed by Zatsiorsky.[44] The lever arm (mass: 15 kg, moment of inertia about the center of mass: 2 kgm^2) was adjusted according to the biomechanical length of the thigh, i.e., the distance between hip and knee joint, yielding a total moment of inertia of about 8.6 kgm^2.

To assess the properties of the apparatus apart from the viscoelasticity of the hip joint, the leg mass was mimicked by a weight attached to the lever arm. Accelerating at $\pm 400°/s^2$ (± 6.981 rad/s^2) to generate a piecewise parabolic movement with an amplitude of 20° (0.349 rad) the motor had to exert rectangular pulses of ±60 Nm which excited oscillations [Fig. 2(a)]. The parameters in Eq. (1) were calculated from the difference between the filtered rectangular acceleration

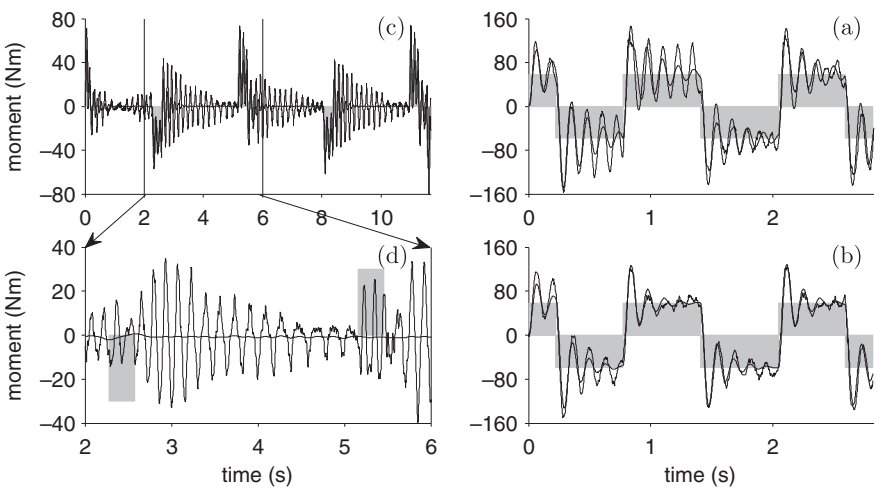

Fig. 2. Determination of the mechanical characteristics of the apparatus and estimation of the contribution of the moment of inertia of leg and lever arm to the recorded moment. (a) Rectangular pulses of ca. ±60 Nm (gray shaded area) acting on a moment of inertia of 8.6 kgm^2 produced an acceleration of $\pm 400°/s^2$ (± 6.981 rad/s^2). The response (thick line) of the transfer function (1) was fitted to the recorded moment (thin line) to evaluate the parameters J, a_1 and a_2.(b) Replacing the equivalent mass by the leg parameters J, a_1 and a_2 were determined applying the pulse sequence in (a).(c) Cyclic movements intended to measure hysteresis effects were generated by shorter pulses (gray shaded area) which started, reversed, and ended motion of the lever arm (e.g., acceleration $\pm 200°/s^2$ [± 3.491 rad/s^2], velocity $\pm 30°/s$ [± 0.524 rad/s], range of motion 70° [1.222 rad] to −15° [−0.262 rad]). The response (thick line) was calculated utilizing the parameters determined before and was subtracted from the recorded moment (thin line). (d) The moment (thin line) that remained yet contained significant oscillations between 5 Hz and 10 Hz, a frequency range not overlapping with the cycle frequencies given in the experiment. Applying a fourth order Butterworth low-pass-filter with a cut-off frequency of 2 Hz almost eliminated these oscillations entirely (thick line).

and the recorded moment using a least-squares optimization method [lsqnonlin, MATLAB optimization toolbox, Fig. 2(a)] yielding $k \approx 20000\,\mathrm{Nm}$, $b \approx 10\,\mathrm{Nms}$, and $J \approx 8.4\,\mathrm{kgm}^2$, the latter being in good agreement with the estimation of J described above.

Substituting the equivalent mass by the leg and conducting of the piecewise parabolic movement [Figs. 2(b) and 3(a)] yielded equivalent results for the parameters J and a_2. Only the parameter a_1 was approximately three times larger which was attributed to the softer coupling between leg and lever arm via the muscles. However, for a cycle with an excursion of 20° around the equilibrium angle generated by a relatively large acceleration the inertial contribution to the total

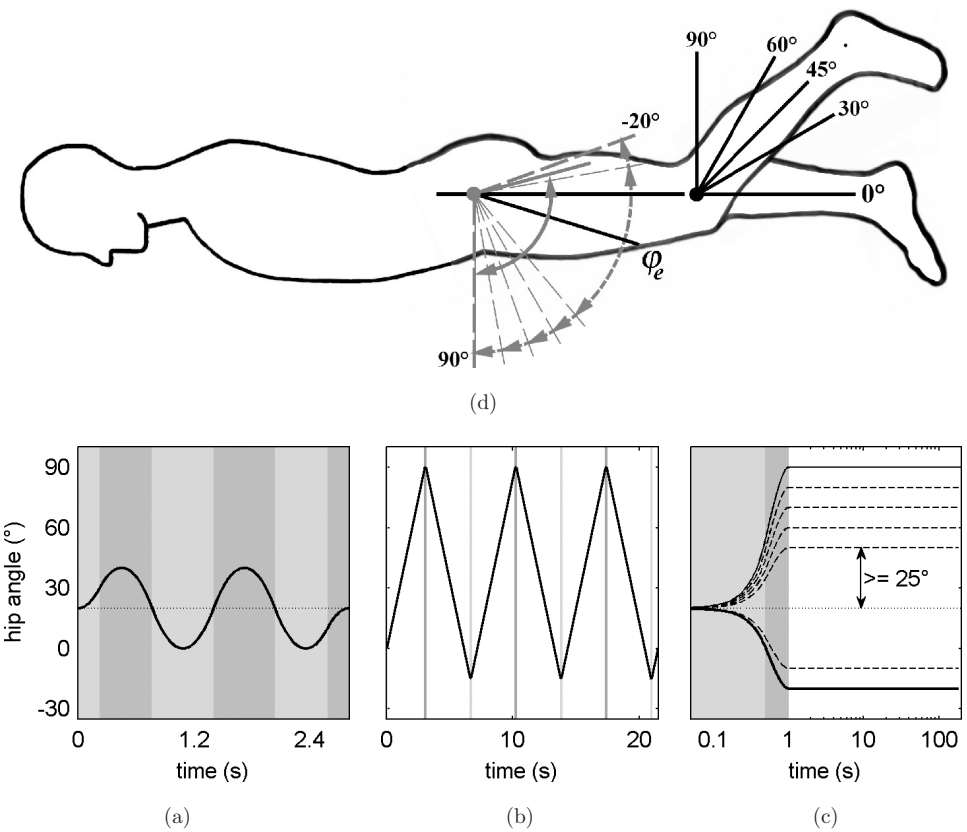

Fig. 3. Motor-driven hip angle-time-courses from the three sections of the experimental protocol: (a) cyclic movement driven at an acceleration of $400°/s^2$ with an amplitude of 20° around the equilibrium angle, (b) triangular wave form of cyclic movements between 90° flexion and −15° extension given to measure hysteresis effects, (c) step-like movements given to measure relaxation, (d) Sketch of the hip range of motion of cyclic movements from −15° extension to 90° flexion (solid gray arc). For step-like movements angles between −20° extension and 90° flexion with a 10° interval (thin dashed gray lines) were target angles. For a recorded equilibrium angle φ_e (example: 18°) only angles with a distance larger than 25° from φ_e were applied in successive trials (indicated by arrows on the dashed gray arc).

recorded moment clearly dominated over the contribution due to passive joint properties. Thus, the parameters J, a_1 and a_2 were conveniently determined per knee angle from an experimental trial with the leg strapped to the lever arm. The moment of inertia J was verified by calculating J from the segment lengths and circumferences as well.

Triangular angle-time-courses applied to measure hysteresis effects contained considerably shorter pulses of acceleration. The response of the transfer function was calculated utilizing the previously determined parameters [Fig. 2(c)] and was subtracted from the recorded moment [Fig. 2(d)]. However, oscillations with frequencies between 5 Hz and 10 Hz remained. These oscillations were generated by exciting modes of higher order due to the nonlinear behavior of the lever arm, which was not covered by the linear transfer function, and resulted in an overestimation of the damping parameter b. Thus, a fourth order Butterworth low-pass-filter with a cut-off frequency at 2 Hz was applied to eliminate these oscillations [Fig. 2(d)].

Finally, the internal friction of the apparatus was evaluated. Internal friction would appear in the recorded signal as constant shift in the moment during movement at constant velocity.[7] If internal friction were present, the mean reduced moment between offset and onset of two acceleration pulses would be nonzero. Taking the direction of movement into account the mean moment estimated at different intervals did not significantly differ from zero (one-sided one-sample t-test, $p > 0.1$), i.e., the apparatus exhibited no internal friction.

2.3. *Experimental procedure*

To measure hysteresis effects and relaxation processes, i.e., viscoelastic behavior of the hip joint, a set of motor-driven cyclic movements at different speeds and step-like movements to several hip joint angles were applied. Joint kinematics was chosen to cover a broad range of velocities to yield an adequate set of data for a model-based description. To avoid involuntary muscle activity the range for the experimental protocol was set below the reported range (Table 1). Maximum hip flexion and extension for cyclic movements were set to 90° and −15°. Targets for a step change in angle were chosen to be between 90° flexion and −20° extension [Fig. 3(d)].

The same number of angle-time-courses were taken for five constant knee angles [0°, 30°, 45°, 60°, and 90°, Fig. 3(d)] presented in a random sequence. All trials at one knee angle were completed in one session. During the course of a session subjects remained on the table but, thereafter, were released from the apparatus for at least one hour before the next session began.

In preparation for the experiment length and circumference of thigh, shank, and foot were measured during upright standing. The biomechanical length of the thigh was calculated from the measured distance between the anterior superior iliac spine and the tibia plateau.[45] The positions of EMG electrodes were marked on the skin as well as the medio-lateral hip joint axis at the cranial end of the greater trochanter.[46] All marks remained throughout the experiment.

At the beginning of each session the skin beneath EMG electrodes was shaved and cleaned with ethanol. Right thigh, pelvis, and upper body were strapped onto the table with the hip joint at 0° and the knee slightly flexed (Fig. 1). The left leg was strapped to the lever arm with the knee extended. The dorsal border of the iliac crest was positioned on a brace to orientate the medio-lateral axis vertically. The drive shaft was aligned with the greater trochanter. To correct for potential misalignment the horizontal position of the table was carefully adjusted monitoring foot movement along the longitudinal axis of the lever during manual rotation.

To ensure that hip joint moments were passively generated the EMG signal of the superficial thigh muscles should not differ from baseline noise. The baseline EMG signal was judged in relation to the EMG signal recorded during isometric maximum voluntary contractions (MVC, Fig. 4). The leg was manually cycled at an approximately constant angular velocity between 90° flexion and −20° extension and finally kept constant at the 0° hip angle. The MVC (one to three sec duration) of the *M. biceps femoris caput longum* and *M. semitendinosus* was measured at full knee extension and the *M. rectus femoris* was contracted with the knee locked at 90° during a consecutive trial. EMG signals were rectified

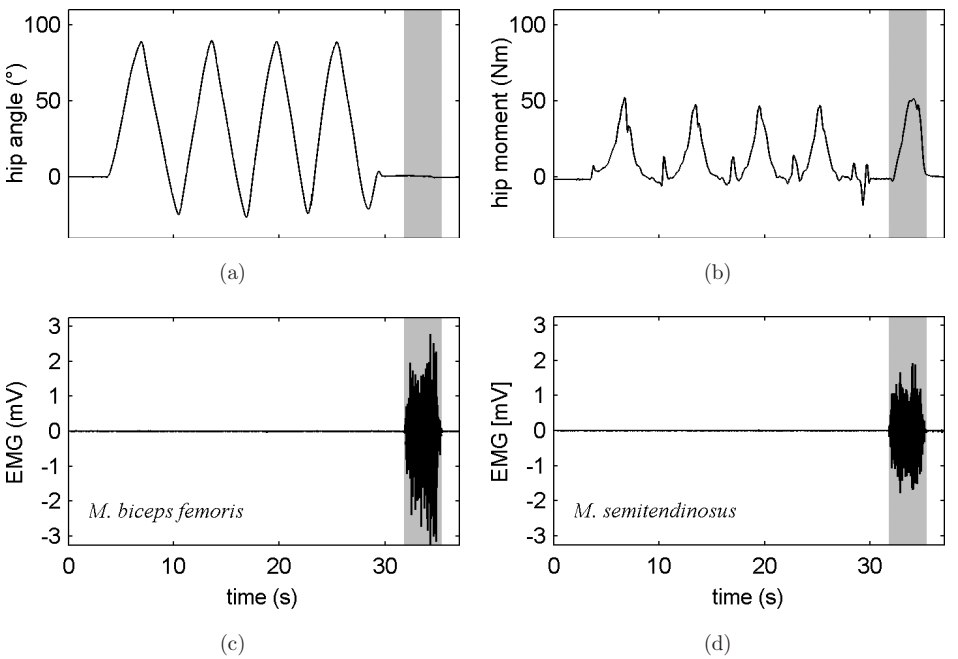

Fig. 4. EMG activity of the hip extensor muscles (*M. biceps femoris*, *M. semitendinosus*) for a cyclic angle time-course between 90° and −20° at ca. ±40°/s. The movement starts and ends at the reference position, 0° hip angle. Voluntary muscle contraction (gray shaded regions) was performed at 0°. (a) hip joint angle; (b) hip joint moment; (c) EMG of *M. biceps femoris* and (d) EMG of *M. semitendinosus*.

and a moving average over a time span of one second was calculated for the non-contraction and the contraction phase separately. The mean baseline noise voltage was less than 1% compared to the mean voltage during MVC. Each of the 13 subjects included in the study did not exhibit muscular activity outside voluntary contractions. Correspondingly, as no noticeable muscle activity was detected in manually driven trials, we concluded that no significant muscle activity was present in the motor-driven experiments as well. EMGs were repeatedly recorded at the beginning of each session to monitor whether subjects were still relaxed and showed no muscular activity.

As the hip joint acts like a nonlinear damped spring system the corresponding equilibrium angle was detected by disengaging the clutch and manually evoking an unrestraint oscillation of the leg. The lever arm came to rest at the equilibrium point which was recorded from the protractor with a precision of 1°.

Subsequently motor-driven movements were presented in three sections. In the first section the piecewise parabolic movement was conducted to assess the leg's moment of inertia and the mechanical properties of the apparatus [Fig. 3(a)].

The second section consisted of a set of 13 trials at which cyclic movements in triangular wave form were given to measure hysteresis effects. During a trial the motor moved the leg for three consecutive cycles between 90° and −15° [Fig. 3(b)]. Each trial was conducted at a different angular velocity (1°/s, 2°/s, 3°/s, 4°/s, 5°/s, 10°/s, 20°/s, 30°/s, 40°/s, 50°/s, 60°/s, 70°/s, and 80°/s) covering a frequency range of approx. two decades (from $4.7 \cdot 10^{-3}$ Hz to $3.4 \cdot 10^{-1}$ Hz). Starting at the reference position the drive shaft accelerated to the given velocity, continued at that velocity, and constantly decelerated to end at the given angle. The triangular form was generated piecewise by instantly inverting acceleration and velocity when the 90° or the −15° angle was hit. The velocities were randomly presented except the velocity of 4°/s which was always presented within the first three trials and was repeated after the third section of each session in order to test for reliability. Between two consecutive trials the leg rested for one minute at the equilibrium angle. The sampling frequency was adjusted to the movement velocity to record approximately the same amount of data per trial (50 to 1000 samples/s, the A/D converter limit).

In the third section, seven trials containing step-like movements were administered to measure relaxation. Subdividing the range between 90° flexion and 20° extension in 10° intervals only angles more than 25° distant from the equilibrium position were given as targets as no significant relaxation was noticed for steps smaller than 25° [Fig. 3(c)]. Starting at the equilibrium angle, the motor accelerated the leg within one second to the target angle, remained for two minutes and returned to the equilibrium angle. After each trial the leg rested for two minutes to allow for viscoelastic structures to recover. The sequence of the target positions was randomized, except for the 80° hip angle which was always presented within the first three trials and repeated at the end of each session to test for reliability. Moments were recorded at 200 samples/s during the third section.

2.4. *Model*

2.4.1. *Characteristics of the QLV theory*

To model the viscoelastic behavior of the hip joint the Quasi-Linear Viscoelastic theory (QLV) proposed by Fung[18] was utilized. The QLV theory assumes on the theory of linear systems that the time-dependent behavior of a material can be described by a normalized reduced relaxation function $h(t)$ so that a response in joint moment $M(\varphi, t)$ to a step change in joint angle φ can be described as the product of a time-independent elastic response $M^e(\varphi)$ and the normalized relaxation function $h(t)$:

$$M(\varphi, t) = h(t) \cdot M^e(\varphi), \quad h(0) = 1. \tag{2}$$

According to the superposition principle the resulting joint moment $M(t)$ can be calculated for an arbitrary input function in joint angle $\varphi(t)$ by means of the convolution integral:

$$M(t) = \int_{-\infty}^{t} h(t-\tau) \frac{\partial M^e}{\partial \varphi} \frac{\partial \varphi}{\partial \tau} \, d\tau. \tag{3}$$

In an experiment the imposed movement usually starts off at zero time. Thus, by assuming $\varphi(t < 0) = 0$ the lower limit can be adjusted to zero:

$$M(t) = M^e(0)h(t) + \int_{0}^{t} h(t-\tau) \frac{\partial M^e}{\partial \varphi} \frac{\partial \varphi}{\partial \tau} \, d\tau. \tag{4}$$

If $M^e(\varphi(t))$ and $h(t)$ are continuously differentiable for $t \geq 0$ expression (4) is equivalent to:

$$M(t) = M^e(t)h(0) + \int_{0}^{t} M^e(\varphi(t-\tau)) \frac{\partial h}{\partial \tau} \, d\tau. \tag{5}$$

2.4.2. *Reduced relaxation function*

To take into account the nonlinear damping behavior of biomaterials Neubert[21] suggested the constant relaxation spectrum $\gamma(\tau) = (\ln(\tau_2/\tau_1))^{-1}$ for $\tau_1 < \tau < \tau_2$ and $\gamma(\tau) = 0$ for $\{\tau < \tau_1, \tau > \tau_2\}$. This spectrum yields the reduced relaxation function:

$$h(t) = 1 + c\left(\frac{\mathrm{E}_1(t/\tau_2) - \mathrm{E}_1(t/\tau_1)}{\ln(\tau_2/\tau_1)} - 1\right) \tag{6}$$

where $\mathrm{E}_1(z) = \int_z^\infty t^{-1} e^{-t} \, dt$ denotes the exponential integral function. The parameter c represents the fraction of relaxation within $h(t)$, i.e., the remaining fraction after complete relaxation is $\lim_{t\to\infty} h(t) = c_0 = 1 - c$. The reduced relaxation function (6) is with the substitution

$$c = \frac{\hat{c} \ln(\tau_2/\tau_1)}{1 + \hat{c} \ln(\tau_2/\tau_1)} \tag{7}$$

equivalent to the reduced relaxation function proposed by Fung[18]:

$$h(t) = \frac{1 + \hat{c}(\mathrm{E}_1(t/\tau_2) - \mathrm{E}_1(t/\tau_1))}{1 + \hat{c}\ln(\tau_2/\tau_1)}. \tag{8}$$

Parameters $\{c, \tau_1, \tau_2\}$ were numerically evaluated using the convolution integral (5) and hence the time derivative of $h(t)$:

$$g(t) = \frac{\partial h}{\partial t} = \frac{c}{\ln(\tau_2/\tau_1)} \frac{1}{t}(e^{-t/\tau_1} - e^{-t/\tau_2}). \tag{9}$$

$g(t = 0)$ was calculated from $\lim_{t\to+0} g(t) = c(\frac{1}{\tau_2} - \frac{1}{\tau_1})(\ln(\tau_2/\tau_1))^{-1}$.

2.4.3. *Elastic response*

An elastic response representing the moment-angle $M^e(\varphi_h)$ of the hip joint has to account for the increase in stiffness $k(\varphi_h) = |\partial M^e/\partial\varphi_h|$ during flexion as well as extension. An exponential functions was frequently used to describe the elastic response.[16,19,29,31,47–49] To represent flexion and extension independently a double exponential function was chosen:

$$M^e(\varphi_h) = -c_1(e^{k_1(\varphi_h-\varphi_0)} - 1) + c_2(e^{-k_2(\varphi_h-\varphi_0)} - 1), \quad \{c_1, c_2\, k_1, k_2 > 0\}. \tag{10}$$

φ_0 denotes the equilibrium angle. The parameters $\{c_1, k_1\}$ and $\{c_2, k_2\}$ describe the joint stiffness. However, to ensure that the function (10) satisfies the condition of minimum stiffness at the equilibrium point the constraint $\partial^2 M^e/\partial{\varphi_h}^2(\varphi_h = \varphi_0) = 0$ was introduced which reduced the amount of free parameters to three:

$$c_2 = -\frac{c_1 {k_1}^2}{{k_2}^2}. \tag{11}$$

2.4.4. *Model parameter estimation and statistics*

After removing the moments caused by the mechanical characteristics of the apparatus from the recorded moment all 13 cyclic and seven step-like angle-time-courses $\varphi_h(t)$ were employed as input functions to the convolution integral (5) to calculate the corresponding output functions $M(t)$. The parameters for $M^e(\varphi_h)$ and $h(t)$ were iterated applying a least-squares optimization method (lsqnonlin, MATLAB optimization toolbox) to minimize the sum of squares of the differences between the calculated and the measured moment-time-courses. Parameters for $M^e(\varphi_h)$ and $h(t)$ were determined per subject and per knee angle, yielding 65 (13 times five) parameter sets.

To get a parameter set for a representative "generic" subject per knee angle the calculated parameters needed to be averaged appropriately by considering characteristic features of the model and the employed functions.

The implementation of a constant relaxation spectrum implicates that the reduced relaxation function has a constant negative linear slope over logarithmic

time between the two time constants[19]:

$$\hat{m} = \frac{dh(t)}{d(\ln t)} = \frac{c}{\ln(\tau_2/\tau_1)}. \tag{12}$$

Therefore the means of the parameters τ_1 and τ_2 and their standard deviations were calculated after logarithmic transformation of τ_1 and τ_2: $\{\ln(\tau_1), \ln(\tau_2)\}$. Mean and standard deviation of the dimensionless constant c were determined without any preceding transformation. The independence of the parameters of the reduced relaxation function permitted to test for their statistical distribution within subjects and to verify potential differences between knee angles.

Because of the interdependence of the three parameters c_1, k_1 and k_2 in representing the stiffness of the joint, a mean parameter set was determined for each knee angle by applying a numerical optimization. The equilibrium angles at the hip joint were averaged over subjects at first. Shifted by the mean equilibrium angle a range from $-20°$ (extension) to $90°$ (flexion) was given to calculate an elastic response per subject. The sum of squares of the difference between the thirteen subject specific elastic responses and the mean elastic response yielded the objective function.

3. Results

3.1. *Hysteresis and relaxation*

To test for reliability the moment-time-courses for the cyclic movement at $4°/s$ and the step-like movement to a hip angle of $80°$ recorded for each subject after the third section of each session were related to the moment-time-courses acquired at the corresponding trials in the second and third section of the protocol. The differences between the curves calculated at each point in time divided by the maximum moment detected yielded a deviation of $2.4 \pm 2.2\%$ (mean $\pm$ s.d.). Therefore, the correlation coefficients ($R^2 > 0.99$) were highly significant ($p < 0.001$).

Recorded and calculated moment-angle-courses, i.e., hysteresis curves from six of thirteen trials, are shown in Fig. 5 for a representative subject with the knee joint adjusted at $45°$. Only minor differences were found among the passive hip joint moments measured for different velocities. The peak moments of the measured hysteresis loops slightly decreased (ca. 15%) from faster to slower movements. The model describes the magnitude and the width of the hysteresis loops. The predicted peak moments tend to decrease faster (ca. 30%) than the measured moments. The deviation between the measured and calculated moment-time-course depended on the direction of movement and gradually increased as the leg moved from the joint boundaries towards the equilibrium angle. The magnitude of the deviation increased with cycle frequency. The area of the model predicted hysteresis loop (ca. 26% of the work done on the joint) was generally smaller than the measured loops (ca. 33%). In principle, a hysteresis loop that has its largest width considerably away from the midrange of a given cyclic movement cannot be matched by the model and would require a different approach.

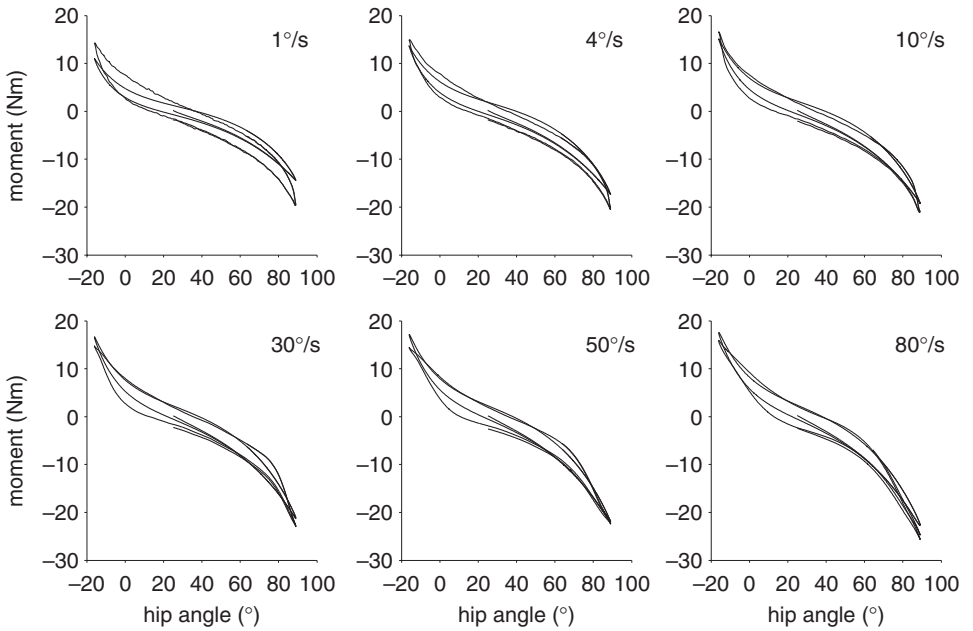

Fig. 5. Hysteresis curves recorded from cyclic movements: Measured (thin line) and calculated (thick line) moment-angle-courses of a representative subject are shown for a sample of six out of thirteen velocities (1°/s, 5°/s, 10°/s, 30°/s, 50°/s, and 80°/s). The knee was fixated at 45° which corresponded to an equilibrium angle of 26° at the hip joint.

For step changes in angle a normalization of the moment-time-courses indicated that the measured rate of relaxation was independent of hip angle [Fig. 6(a)]. The observed relaxation of the joint moment over time after a step acceleration within one second to different angles [Fig. 6(b)] were lower than the slopes $\hat{m}$ (12) based on the calculated time constants. As can be seen from the relatively large difference between the ramp time of one second and the calculated values for τ_1 the effect of the moments from the step-like movements on determining τ_1 during parameter calculation was small.

3.2. *Reduced relaxation function*

A boxplot of the parameters c, $\ln \tau_1$ and $\ln \tau_2$ indicates a low skewness (Fig. 7). Parameter values were normally distributed ($p < 0.05$) per knee angle. Means and standard deviations are shown in Table 2. A two-way analysis of variance computed for each parameter revealed no significant differences for subjects but a significant contribution of the knee angle to c and $\ln \tau_2$. A subsequently applied multiple comparison test (Tukey-Kramer method) showed some significant differences between combinations of knee angles ($p < 0.05$) which did not indicate a systematic trend (Fig. 7).

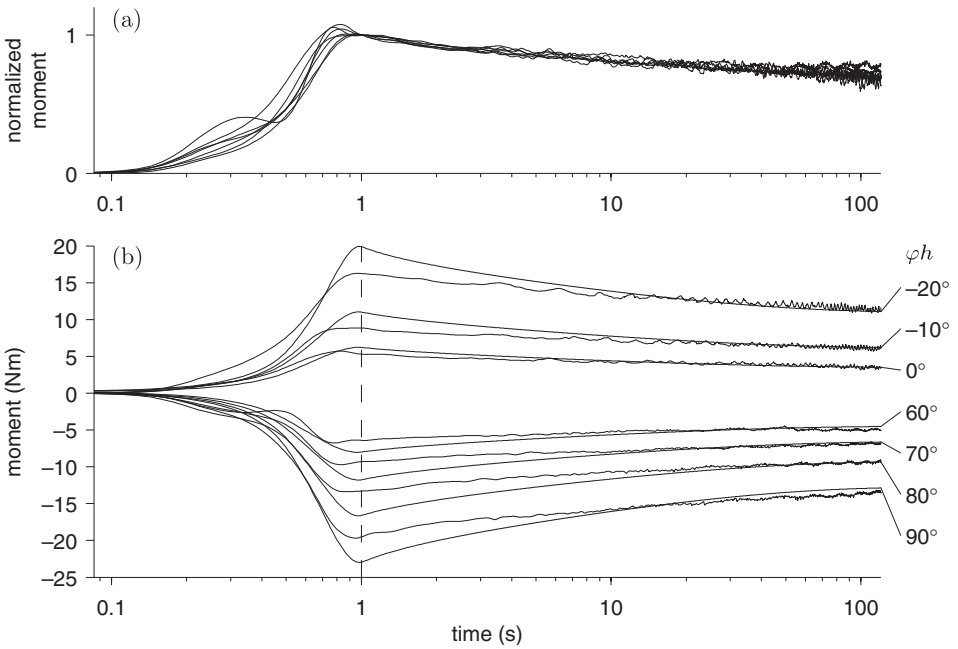

Fig. 6. Relaxation occurring after steps to seven different hip angles φ_h, indicated on the right, starting at an equilibrium angle of 26° (45° knee angle). (a) Normalization by the moment measured at the time of one second demonstrated that rate of relaxation was independent of hip angle. (b) Measured (thin line) and calculated (thick line) moment-[logarithmic time]-courses of a representative subject (as in Fig. 5). For comparison: The relaxation spectrum was estimated as being within $\tau_1 = 0.115\,\mathrm{s}$ and $\tau_2 = 66.24\,\mathrm{s}$.

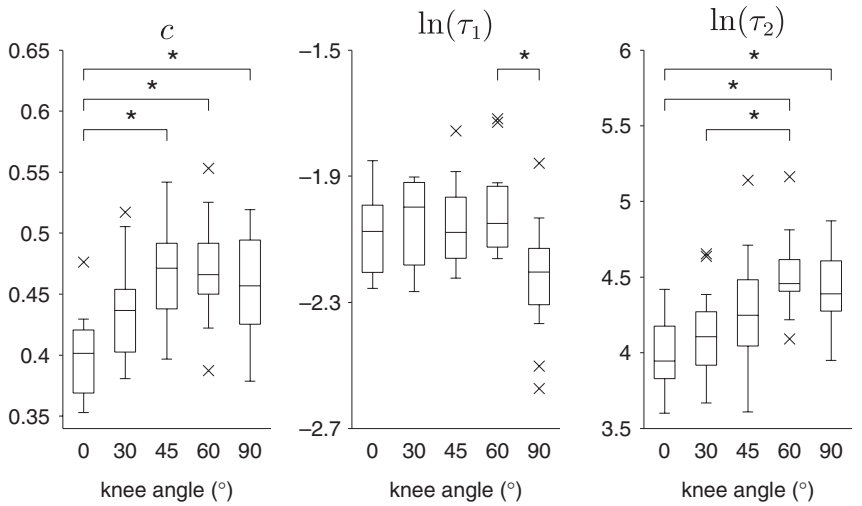

Fig. 7. Parameters c, $\ln\tau_1$ and $\ln\tau_2$, of the reduced relaxation function for all subjects: The box indicates lower quartile, median, and upper quartile. The whiskers show the range and the crosses represent values outliers (>three quartile distances). A multiple comparison test (Tukey-Kramer method) revealed some significant differences ($p < 0.05$) between knee angles indicated by the stars.

Table 2. Mean and standard deviation of the calculated parameters c, τ_1 and τ_2, of the reduced relaxation function per knee angle respectively and one comprehensive parameter set.

Knee angle (degree)	c	$\ln \tau_1$	$\ln \tau_2$
0	0.399 ± 0.035	-2.081 ± 0.136	3.977 ± 0.239
30	0.436 ± 0.042	-2.054 ± 0.142	4.110 ± 0.311
45	0.468 ± 0.039	-2.052 ± 0.135	4.296 ± 0.382
60	0.471 ± 0.043	-2.005 ± 0.146	4.523 ± 0.266
90	0.456 ± 0.041	-2.225 ± 0.186	4.428 ± 0.247
φ_{ki}	0.446 ± 0.047	-2.083 ± 0.164	4.267 ± 0.349

Note: For the time constants τ_1 and τ_2 mean and standard deviation were calculated after calculation of the logarithm.

As the frequency range of the given input functions was the same for all knee angles the range of relaxation times was assumed to be not significantly different with respect to the knee angles. Noted differences were attributed to the asymmetric size of the flexion and extension ranges, i.e., the range from the equilibrium angle to the boundaries, so that the weight of flexion and extension moments on the determination of the model parameters altered with knee angle. According to the rather consistent results found for the knee angles a "generic" parameter set for c, $\ln \tau_1$ and $\ln \tau_2$, added as final row to Table 2, was calculated from all five times 13 parameters respectively (Fig. 8).

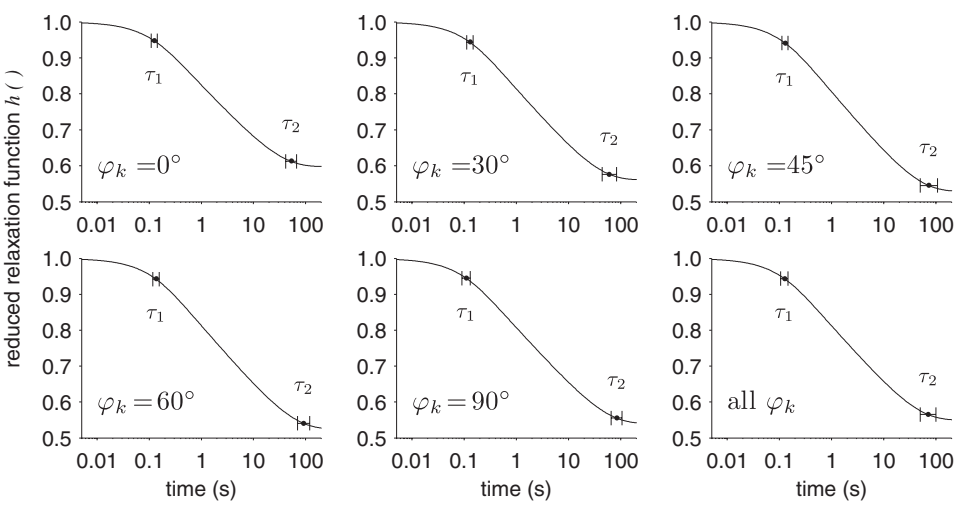

Fig. 8. Logarithmic time courses of the mean reduced relaxation functions $h(t)$ for the five knee angles as well as for a generic function including the optimization results of all knee angles φ_k, circles and vertical bars indicate mean and the standard deviation of the logarithmically transformed time constants τ_1 and τ_2 shown in Table 2.

3.3. *Equilibrium angle at the hip joint*

The measured equilibrium angles φ_0 (Table 3, last column) were normally distributed for each knee angle respectively ($p > 0.05$). As expected the equilibrium position at the hip joint continuously increased with knee flexion (Fig. 9). A multiple comparison test revealed significant differences ($p < 0.05$) between all knee angles except for directly adjacent angles. An exponential function of the form:

$$\varphi_0(\varphi_k) = \tilde{a}_0 + a_0(1 - e^{-a_1\varphi_k}), \quad \{\tilde{a}_0, a_0, a_1 > 0\}. \tag{13}$$

($\tilde{a}_0 = 9.36°$, $a_0 = 38.67°$, $a_1 = 0.0132$) yielded a distinctly better regression as the linear relationship $\varphi_0(\varphi_k) = \tilde{b}_0 + b_1\varphi_k$ ($\tilde{b}_0 = 11.6°, b_1 = 0.3$). The norm of the residuals calculated for the exponential function amounted to only 3% of the norm for the linear function.

Table 3. Mean parameter sets for the elastic responses calculated for each knee angle and one parameter set determined over all knee angles. Mean and standard deviation (mean ± s.d.) of the measured equilibrium angles are given in the last column.

	Branch for hip flexion		Branch for hip extension		
Knee angle (degree)	c_1 (Nm)	k_1 (1/rad)	c_2 (Nm)	k_2 (1/rad)	Equilibrium angle φ_{0i} (degree)
0	3.836	2.109	3.132	2.334	9.5 ± 5.0
30	4.902	1.854	1.39	3.481	22.2 ± 3.4
45	5.72	1.672	1.163	3.707	26.1 ± 2.8
60	5.195	1.751	1.385	3.392	31.1 ± 3.2
90	5.532	1.669	1.351	3.376	36 ± 2.9
φ_{ki}	3.67	2.137	1.497	3.345	$\varphi_{0i}(\varphi_{ki})$

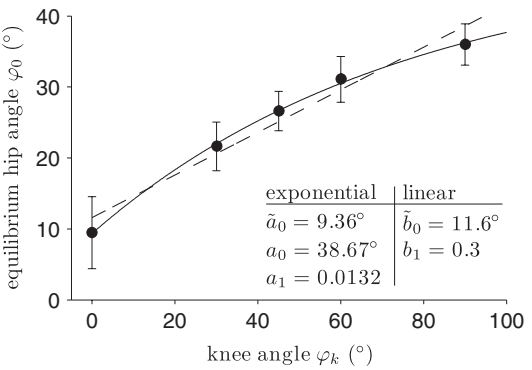

Fig. 9. Means (dots) and standard deviation (bars) of the equilibrium angles φ_{0i} measured at the knee angles (φ_{ki}). Exponential (solid line; Eq. (13)) and linear (dashed line) regression for gaining a continuous relationship between knee angle and equilibrium angle at the hip joint. Regression results are shown at the inset table.

3.4. *Elastic response*

The stiffness characteristics of the mean elastic responses calculated per knee angle only differed minimally (Fig. 10). The double exponential function (10) was essentially shifted with respect to the hip joint angle. In conjunction with the relationship $\varphi_0(\varphi_k)$ between knee and equilibrium angle all (five times 13) elastic responses were taken as input functions to attain an overall parameter set $\{c_1, c_2, k_1, k_2\}$ yielding an elastic response $M^e(\varphi_h, \varphi_k)$ as function of hip and knee angle:

$$M^e(\varphi_h, \varphi_k) = -c_1(e^{k_1(\varphi_h - [\tilde{a}_0 + a_0(1-e^{-a_1\varphi_k})])} - 1) + c_2(e^{-k_2(\varphi_h - [\tilde{a}_0 + a_0(1-e^{-a_1\varphi_k})])} - 1). \quad (14)$$

The functions $M^e(\varphi_h)$ determined from the respective parameter sets for each knee angle and the function $M^e(\varphi_h, \varphi_k)$ calculated for $\varphi_k = (0°, 30°, 45°, 60°, 90°)$ are in good agreement and deviations are small (Fig. 11).

Scaling of the elastic response by subject specific mass and length parameters in order to gain a dimensionless function did not reduce the differences between subjects. Therefore, the dimension of the elastic response was kept in Nm.

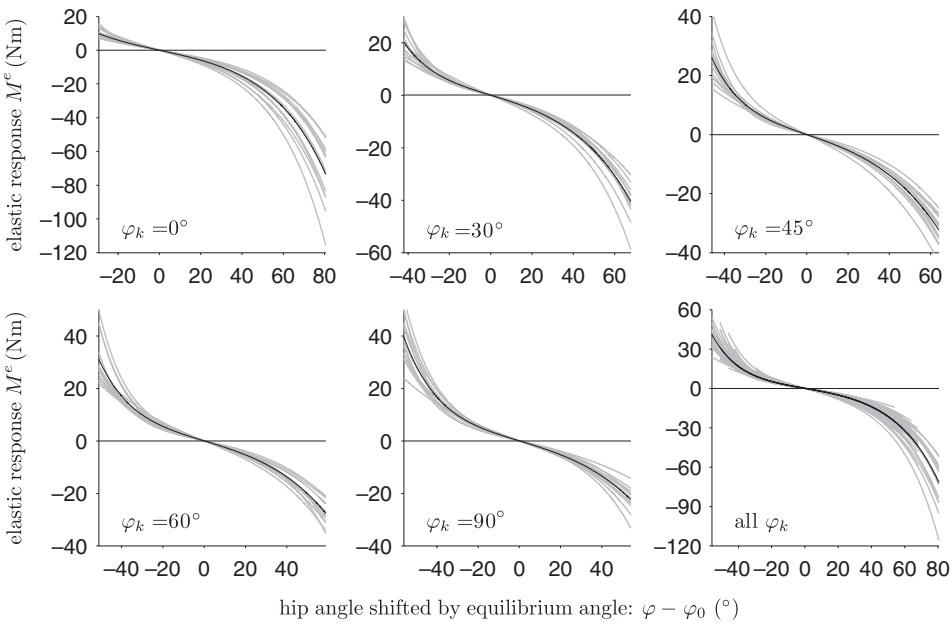

Fig. 10. Mean elastic responses per knee angle determined by nonlinear optimization. The hip range of motion from −20° extension to 90° flexion respectively shifted by the mean equilibrium angle was used to calculate the thirteen subject specific elastic responses which were given as numerical input. Finally, one parameter set resulted from all 65 functions.

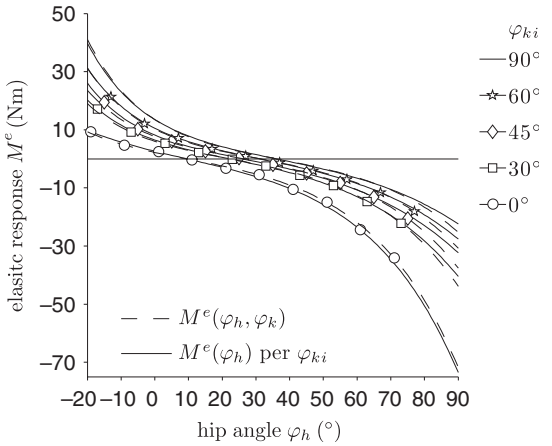

Fig. 11. Deviation between functions $M^e(\varphi_h)$ determined per knee angle and function $M^e(\varphi_h, \varphi_k)$ calculated for $\varphi_k = (0°, 30°, 45°, 60°, 90°)$. Parameter set for $M^e(\varphi_h, \varphi_k)$: $c_1 = 3.67\,\text{Nm}$, $c_2 = 1.497\,\text{Nm}$, $k_1 = 2.137\,\text{rad}^{-1}$, $k_2 = 3.345\,\text{rad}^{-1}$ (as in Table 3) and $\tilde{a}_0 = 0.1634\,\text{rad}$, $a_0 = 0.675\,\text{rad}$, $a_1 = 0.756\,\text{rad}^{-1}$ (parameters from Fig. 9 in radians). φ_k and φ_h need to be in radians for calculation of $M^e(\varphi_h, \varphi_k)$.

4. Discussion

We built an experimental apparatus in order to measure moment-angle-relations for a set of defined joint velocities. A servo motor allowed for precise control of cyclic and step-like movements of the hip joint, and captured the damping behavior well. This is difficult to accomplish during manually controlled experiments. Corresponding studies often did not account for damping effects and focused merely on the passive elastic properties of the joint.[14,16]

In our experimental setup the leg's moment of inertia inevitably contributed to the recorded signal during acceleration phases. The mechanical characteristics of the apparatus and the leg's moment of inertia were approximated by a linear second order transfer function, which allowed to separate moments due to the inertial and mechanical properties of the apparatus from relevant moments originating from the viscoelastic properties of the joint. As a consequence, we utilized complete hysteresis loops and relaxation-time-courses to comprehensively describe the damping characteristics of the hip joint, while other studies had to exclude data segments from analysis due to the predominance of inertial or frictional effects.[7,15]

The moment-time-courses measured during step-like and cyclic movements showed characteristics that can properly be described by QLV theory. Regarding step-like changes in angle the observed rate of relaxation was independent of hip joint angle. This result on the macroscopic level is supported by similar findings on structures constituting the hip joint, in particular ligaments[26,27] and muscles.[22,23] However, further studies on ligaments reported both increasing[31] and decreasing rates[32,50] of relaxation with respect to level of strain. Diverse findings were attributed to disparate measurement protocols that varied in strain level and strain

rate.[51] Some studies on collagenous tissues[28,30] and muscles[25] only applied one level of strain and, therefore, did not measure any effect of strain level on the rate of relaxation.

The hysteresis loops during cyclic movements barely changed over the range of given joint velocities[6] confirming that the rate-insensitivity of the hysteresis loop is a salient feature of the underlying biological tissues.[18] A significant hysteresis effect was already observed for rates distinctly slower than joint velocities during human locomotion. This observation casts doubt on the assumption, that damping effects can be neglected under "quasi-static" movement conditions.[14] The shape of the hysteresis was comparable to the passive viscoelastic behavior of muscle, resulting in a similar divergence between the measured and the predicted loop.[25] The measured loss of energy for muscle (35%−44%)[25] was slightly larger than that for the hip joint (ca. 33%). The measured peak moments increased with joint velocity (ca. 15%) indicating a minor "stiffening"-response. With respect to a frequency range of two decades this amount of "stiffening" has been observed for ligaments (<20%) as well.[19,31] However, experimental results referring to "stiffening" of biological tissues during cyclic loading vary widely.[28,24,25] Accordingly, the properties of the hip joint seem to originate from the viscoelastic properties of the joint capsule including ligaments, and muscles. Both structures contribute more than 40% to the overall stiffness of a joint.[52] Muscles potentially dominate the viscoelastic response due to their arrangement. Hip flexion is mainly restricted by biarticular muscles, such as *M. biceps femoris caput longum* and *M. semitendinosus*. Hip extension is limited by the *M. rectus femoris* and the joint capsule with the covering ligaments. The relative contribution of the connective tissue increases with knee extension as all four major ligaments (*L. iliofemorale*, *L. pubofemorale*, *L. ischiofemorale*, *and Zona orbicularis*) are strained towards hip extension.[53]

4.1. *Reduced relaxation function*

The window of relaxation times is largely determined by the frequency and the time window (two minutes for step change in hip angle) provided by the input kinematics. Quantification of the time constant τ_1 is primarily bound to the upper limit of the frequency range. With respect to the relatively large leg mass the upper limit of the frequency range for motor driven movements was set by the capability of the experimental apparatus. That is, the frequency range of the imposed kinematics must not overlap with the frequency of the oscillations caused by the mechanical characteristics of the apparatus. The fastest cyclic movements within our experimental procedure corresponded to a frequency of $3.4 \cdot 10^{-1}$ Hz hence to a time constant of 0.47 s. As it is known that the damping covered by the reduced relaxation function drops at τ_1 (as well as at τ_2) to about the half of the maximum at mid-frequency [21] the magnitude anticipated for τ_1 should be smaller than 0.47 s in order to describe the hysteresis of the fastest cycle properly. Using the convolution integral (5) for the numerical evaluation the lower limit for τ_1 is confined to the

temporal resolution of the recorded signal, hence τ_1 cannot be smaller than 10^{-3} s *a priori*. At the same time, the temporal resolution of the recorded signal, which was two orders in magnitude (10^2) larger than the corresponding time of 0.47 s, provided an acceptable data basis to evaluate time constants in the vicinity of 10^{-1} s reasonably well.

The magnitudes of parameter τ_1 determined by the optimization process were considerably less than the given ramp time which seems to be necessary in order to describe the contributions of the fast changes in joint moment occurring during ramp time. During numerical evaluation of the time parameters the flattening of $h(t)$ for times larger than τ_2 compensated for the overestimation of the negative slope in the early portion of the moment-time-courses so that the calculated value for parameter τ_2 was smaller than the duration relaxation was recorded. Due to the interdependence of relaxation and hysteresis an overestimation of the negative slope (Fig. 6) accompanied by a faster decrease in the predicted peak moment (Fig. 5) can be regarded as an implication to match the width of the hysteresis loops properly. By exploiting the features of the QLV model and especially those of the reduced relaxation function, the parameters c, τ_1 and τ_2 can interdependently recalculated preferably around their mid-frequency and within the constraint $0 < c < 1$ to potentially compensate for the discrepancy between the slope of the measured and calculated moment-time-courses (compare Sauren and Rousseau[54] who used the parameter $\hat{c}$ instead of c (see Eq. (7)).

The phase angle

$$\psi_m = \tan^{-1}\left\{c\left[\tan^{-1}\left(\sqrt{\frac{\tau_2}{\tau_1}}\right) - \tan^{-1}\left(\sqrt{\frac{\tau_1}{\tau_2}}\right)\right]\left[\left(1 - \frac{c}{2}\right)\ln\frac{\tau_2}{\tau_1}\right]^{-1}\right\} \qquad (15)$$

and the absolute value of the constant negative slope $\hat{m}$ are functions of the ratio τ_2/τ_1 and c at mid-frequency $\omega_m = (\sqrt{\tau_1\tau_2})^{-1} = {\tau_m}^{-1}$ respectively. A symmetric increase of the ratio τ_2/τ_1 around the mid-frequency by multiplying τ_1 with 10^{-2} and τ_2 with 10^2, for instance, results in a shift of the parameter c to 0.8 in order to retain the phase angle ψ_m [Fig. 12(a)].

Simultaneously, the slope $\hat{m}$ at mid-frequency decreases as intended. Shifting the time constants τ_1 and τ_2 to smaller and larger values respectively expands the frequency range where damping effects are covered by the model and, thus, enhances the applicability of the model (see below: application to human locomotion). According to the QLV theory the reduced relaxation function is a normalized dimensionless function of time and has to satisfy the constraint $h(t = 0) = 1$. Varying the parameters of the reduced relaxation function alone does not maintain the initially determined damping characteristics. Fortunately, this can be properly adjusted due to the interaction of the reduced relaxation function and the elastic response within the convolution integral by scaling the elastic response with the factor $h(\tau_m)/h(\tilde{\tau}_m)$ [Fig. 12(a)]. Utilizing the recalculated parameters for the reduced relaxation function and the scaled elastic response the measured hysteresis loops can be described as before [Figs. 12(c), 12(d) and 5]. The inclination of

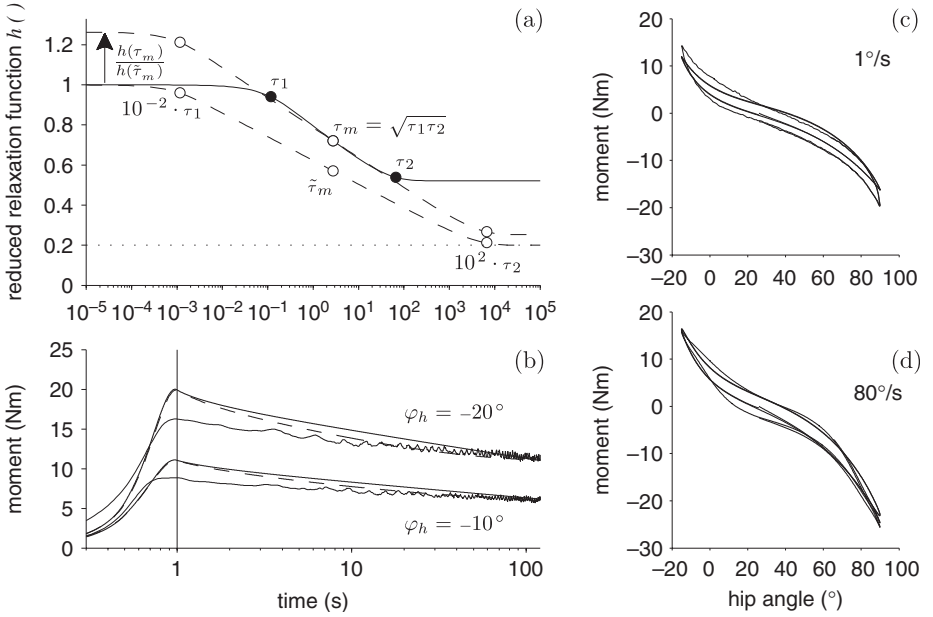

Fig. 12. Determination of an equivalent parameter set c, τ_1 and τ_2 by exploiting characteristics of a constant relaxation spectrum at mid-frequency ω_m in order to potentially compensate for observed differences between measured and calculated moment-time-courses. (a) First, τ_1 and τ_2 were multiplied by 10^{-2} and 10^{2} respectively. As the phase angle ψ_m at mid-frequency and the constant negative slope $\hat{m}$ can be treated as functions of the ratio τ_2/τ_1 and c parameter c was adjusted to 0.8 accordingly. Finally, in order to maintain the constraint $h(t = 0) = 1$, the elastic response was scaled by the factor $h(\tau_m)/h(\tilde{\tau}_m)$. (b) Relaxation (thin solid line) measured for steps to hip angles φ_h of $-10°$ and $-20°$ starting at the equilibrium angle (26°; knee angle: 45°). Remaining lines show the difference between the slopes of the originally calculated response (dashed line, as in Fig. 6) and the response calculated for the shifted parameter set (thick solid line). (c), (d) Measured (thin line) and calculated (thick line) hysteresis loops using the shifted reduced relaxation function and the scaled elastic response: Results are shown for the slowest (1°/s) and fastest (80°/s) velocity imposed during cyclic movements (knee angle: 45°; equilibrium angle at the hip joint: 26°).

the step responses diminished slightly, but the slopes of the measured moment-time-courses were too small to be matched properly [Fig. 12(b)]. Even a maximum shift of parameter c close to 1 did not sufficiently decrease the slope under the constraint of maintaining the width of the hysteresis loops. When taking only the relaxation data as input functions for parameter evaluation the model described the moment-time-courses well by a combination of a large ratio τ_2/τ_1 and a small parameter c which resulted, however, in a considerable underestimation of the hysteresis loops. Furthermore, the applied parameter variation could not account for the overestimation of the moments predicted at ramp time. In consequence, the damping characteristics observed for cyclic and step-like joint kinematics could not entirely match within the QLV modeling approach by utilizing a constant relaxation spectrum suggested by Fung.[18]

For an accurate prediction of very low values for τ_1 the temporal resolution of the reduced relaxation function $h(t)$ and its time derivative $g(t)$ (Eq. (9)) needs to be approximately an order of magnitude (10^1) higher as the expected value for τ_1 (usually close to the ramp time for step chances) so that the numerical error within the convolution (Eq. (5)) is low and can be neglected. This has the disadvantage that the application of the convolution integral for numerical evaluation of all parameters becomes computational very expensive for long time series and large ratios τ_2/τ_1.

4.2. *Elastic response*

The double exponential function was suitable to describe the elastic characteristics of the hip joint, i.e., the continuously increasing stiffness towards flexion as well as extension. The stiffness of the hip joint depends on biarticular muscles spanning hip and knee joint. We accounted for this effect by repeating the measurements at the hip joint for a discrete number of knee angles. The five elastic responses calculated per knee angle virtually showed the same stiffness characteristics merely shifted by a constant hip angle. Similar results were found in studies[6,7,16] excluding moments caused by the gravitational force from the recorded signal. Studies in which the gravitational force contributed to the measured moment during leg movement claimed that the flexor moment at the hip joint was insensitive to knee angle.[14,15] But as the biarticular rectus femoris lengthens with knee flexion the flexor moment at the hip joint should continuously increase with knee angle. Therefore, the passive flexor moment-angle-relationship for the hip joint may be biased by the experimental setup and the calculation procedures in the latter studies.

We did not separately introduce an elastic response function per agonistic muscle group and not differentiate between uniarticular and biarticular muscles.[16,3] This seems to be a reasonable approach for the hip joint due to the consistent stiffness characteristics over all knee angles. Merely establishing a functional relation between the equilibrium angle at the hip joint and the knee joint already yielded a proper elastic response as function of hip and knee angle described by only six free parameters which makes a further application convenient.

Drawback in the determination of the parameters of the elastic response was that the range of motion was not symmetrically selected around the equilibrium angle, so especially the extension branch in the 0° knee angle was quite narrow for parameter estimation.

4.3. *Application to human locomotion*

Our model can be applied to estimate the contribution of passive joint moments during human locomotion which was already done using an elastic model.[3] A merely elastic function is easier to handle but does always overestimate the energy gained from passive structures.

We calculated the hip angle-time-course and the knee angle-time-course for a gait cycle from published kinematic data[55] (Fig. 13). The angle-time-course of the equilibrium angle at the hip joint was calculated from Eq. (13). The hip and knee angle-time-courses were taken as input functions to the convolution integral (Eq. (5)). Furthermore, the shifted parameter set for the reduced relaxation function and the scaled elastic response from Table 3 (last row) were applied. Figure 14 shows the passive hip joint moments estimated. The clockwise direction of the moment-hip angle-loop indicates a gain of energy by a transfer from knee to hip joint via biarticular muscles.[16] In order to calculate the energy absorbed by viscoelastic structures during the course of the gait cycle the passive joint moment needs to be evaluated with respect to the effective hip angle which is the difference between the hip angle and the equilibrium angle. According to the theory the elastic response shows no hysteresis and thus no prediction of energy loss [Fig. 14(b)]. The time derivative of the effective hip angle multiplied by the calculated passive joint moment yields the contribution of passive structures to the joint power during gait. Integrating over time, the negative areas yielded the energy absorbed and the positive areas summarized the energy gained [Fig. 14(c)]. The model calculated that the energy returned by passive structures amounts to 73% of the work done on the

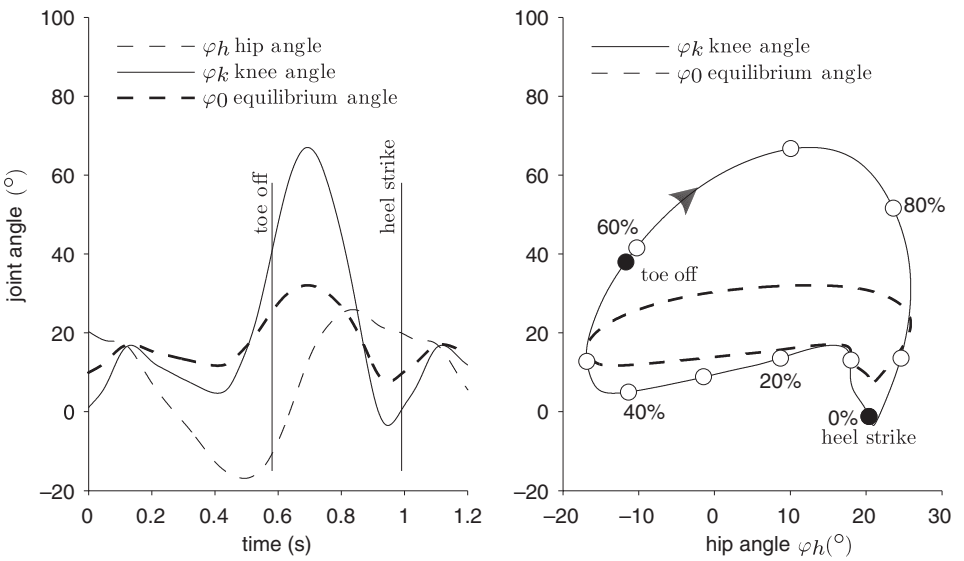

Fig. 13. Kinematic data of human gait: (a) Hip angle-time-course (dashed line), knee angle-time-course (solid line), time-course (thick dashed line) of the equilibrium angle at the hip joint calculated from Eq. (13). The gait cycle start with the heel strike. (b) Knee angle-hip angle loop (solid line) and equilibrium angle-hip angle loop (thick dashed line). White circles mark the joint angle position as percentage of gait cycle and black dots mark the beginning of stance and swing phase.

joint which should be considered as the upper limit due to the underestimation of the experimentally determined hysteresis loops.

The calculated peak moment at toe-off is considerably smaller (≈65%) than the peak moment predicted by Silder *et al.*[16] Taking the published parameter set for the elastic hip joint function and calculating thereof the equilibrium angle-knee angle relation from their elastic function for the hip joint the result shows a considerable shift (10°−15°) of the equilibrium angle towards hip flexion which comprises the major difference within the results of both experiments. The same shift of the

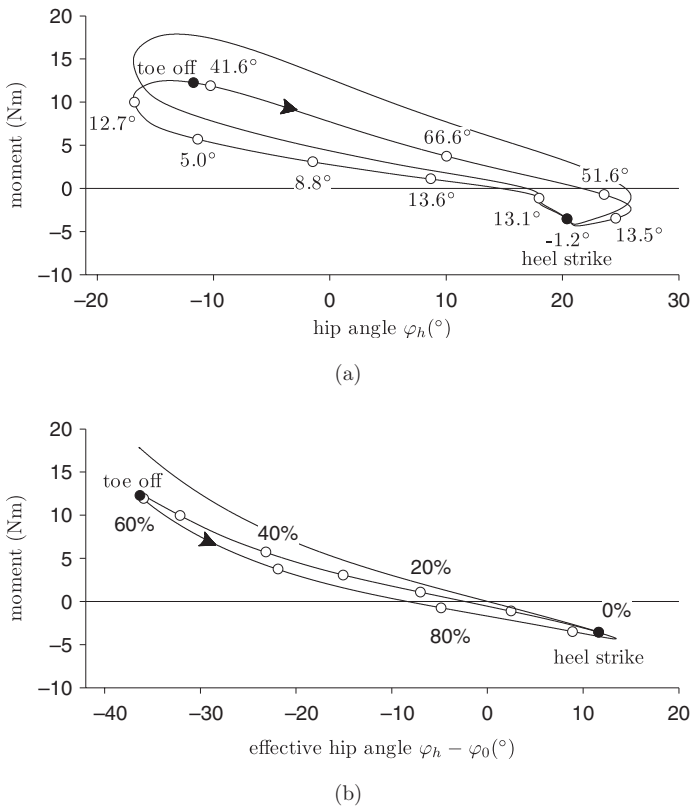

Fig. 14. Estimation of the contribution of passive structures to the hip joint moment during human gait and estimation of the energy loss within a gait cycle due to the viscoelastic joint properties: Circles divide the gait cycle in 10% segments starting at heel strike (as in Fig. 13). (a) Passive hip joint moment-[hip angle]-loops: elastic response (thin line) as the theoretical upper limit of the viscoelastic model, the estimated joint moment (thick line). Loops are passed through in clockwise direction indicating an energy transfer from the knee joint to the hip joint via biarticular muscles. Values in degree at every circle show the corresponding knee angle position. (b) Passive hip joint moment − "effective" hip angle − loop: elastic response $M^e(\varphi_h, \varphi_k)$ (thin line), estimated joint moment $M(\varphi_h, \varphi_k, t)$ (thick line). The effective hip angle gives the difference between the hip joint angle and the equilibrium angle. The hysteresis loop is now run through in counterclockwise direction. (c) Passive joint power calculated from the time derivative of the effective hip angle and the passive hip joint moment: the ratio of the sum of the positive areas (the energy gained) divided by the sum of the negative areas (the work done) is 73%.

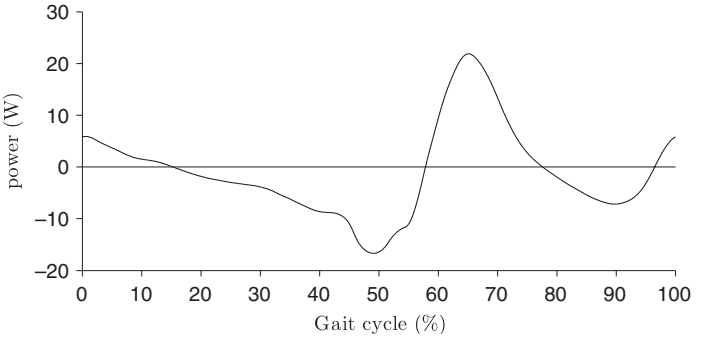

(c)

Fig. 14. (*Continued*)

equilibrium angle at the hip joint was implicitly reflected in the conclusion that passive properties are particularly utilized during the second half of the stance phase and the first half of the swing phase.[3] Our calculation of the passive hip joint power within a gait cycle [Fig. 14(c)] shows that during late swing work is done to passively stretch the hip extensors and subsequently energy is returned during leg retraction in late swing and early stance. Therefore, passive properties are cyclically exploited in both directions of movement not only during leg extension.

The demonstrated enhancement of the ratio τ_2/τ_1 and the corresponding adjustment of the parameter c were necessary to discuss the application of the model to human movement. The cycle frequency of the gait cycle is larger than the maximum frequency applied within the experimental protocol. Therefore, the originally determined parameter τ_1 within the reduced relaxation function (Table 2) would have been too high for a proper calculation of the passively absorbed energy during human gait. Further optimization of test apparatus and data processing will allow measurements in a range comprising those frequencies typical for human walking and running and will help to pinpoint the contributions of viscoelastic tissue properties to the dynamics and energetics of human locomotion and to experimentally verify our calculations.

Acknowledgments

This work was supported by the German Science Foundation (DFG) grants INK 22/B1-1 (B2). Thanks to Dagmar Sternad for personal advice and kind support.

References

1. Saibene F, Minetti A, Biomechanical and physiological aspects of legged locomotion in humans, *Eur J Appl Physiol* **88**:297–316, 2003.

2. Marsh RL, Ellerby DJ, Carr JA, Henry HT, Buchanan CI, Partitioning the energetics of walking and running: Swinging the limbs is expensive, *Science* **303**:80−83, 2004.
3. Whittington B, Silder A, Heiderscheit B, Thelen DG, The contribution of passive-elastic mechanisms to lower extremity joint kinetics during human walking, *Gait Posture* **27**:628−634, 2008.
4. Cavanagh PR, *Biomechanics of Distance Running*, Human Kinetics, Champaign, 1990.
5. Winter DA, Moments of force and mechanical power in jogging, *J Biomech* **16**:91−97, 1983.
6. Yoon YS, Mansour JM, The passive elastic moment at the hip, *J Biomech* **15**:905−910, 1982.
7. Vrahas MS, Brand RA, Brown TD, Andrews JG, Contribution of passive tissues to the intersegmental moments at the hip, *J Biomech* **23**:357−362, 1990.
8. Mansour JM, Audu ML, The passive elastic moment at the knee and its influence on human gait, *J Biomech* **19**:369−373, 1986.
9. Esteki A, Mansour JM, An experimentally based nonlinear viscoelastic model of joint passive moment, *J Biomech* **29**:443−450, 1996.
10. McFaull SR, Lamontagne M, *In vivo* measurement of the passive viscoelastic properties of the human knee joint, *Hum Mov Sci* **17**:139−165, 1998.
11. Gottlieb GL, Agarwal GC, Dependence of human ankle compliance on joint angle, *J Biomech* **11**:177−181, 1978.
12. Weiss PL, Kearney RE, Hunter IW, Position dependence of ankle joint dynamics I. Passive mechanics, *J Biomech* **19**:727−735, 1986.
13. Hoang PD, Gorman RB, Todd G, Gandevia SC, Herbert RD, A new method for measuring passive length-tension properties of human gastrocnemius muscle *in vivo*, *J Biomech* **38**:1333−1341, 2005.
14. Riener R, Edrich T, Identification of passive elastic joint moments in the lower extremities, *J Biomech* **32**:539−544, 1999.
15. Amankwah K, Triolo RJ, Kirsch R, Effects of spinal cord injury on lower-limb passive joint moments revealed through a nonlinear viscoelastic model, *J Rehabil Res Dev* **41**:15−32, 2004.
16. Silder A, Whittington B, Heiderscheit B, Thelen DG, Identification of passive elastic joint moment-angle relationships in the lower extremity, *J Biomech* **40**:2628−2635, 2007.
17. Anderson DE, Nussbaum MA, Madigan ML, A new method for gravity correction of dynamometer data and determining passive elastic moments at the joint, *J Biomech* **43**:1220−1223, 2010.
18. Fung YC, *Biomechanics: Mechanical Properties of Living Tissues*, Springer, Berlin, 1993.
19. Woo SL-Y, Gomez MA, Akeson WH, The time and history-dependent viscoelastic properties of the canine medial collateral ligament, *J Biomech Eng* **103**:293−298, 1981.
20. Drapaca CS, Sivaloganathan S, Tenti G, Nonlinear constitutive laws in viscoelasticity, *Math Mech Solids* **12**:475−501, 2007.
21. Neubert HKP, A Simple Model Representing internal damping in solid materials, *Aeronaut Q* **14**:187−210, 1963.
22. Pinto JG, Fung YC, Mechanical properties of the heart muscle in the passive state, *J Biomech Eng* **6**:597−616, 1973.
23. Pinto JG, Patitucci PJ, Visco-elasticity of passive cardiac muscle, *J Biomech Eng* **102**:57−61, 1980.
24. Blickhan R, Stiffness of an arthropod leg joint, *J Biomech* **19**:375−384, 1986.

25. Best TM, McElhaney J, Garrett WE, Myers BS, Characterization of the passive responses of live skeletal muscle using the quasi-linear theory of viscoelasticity, *J Biomech* **27**:413−419, 1994.
26. Lucas SR, Bass CR, Salzar RS, Oyen ML, Planchak C, Ziemba A, Shender BS, Paskoff G, Viscoelastic properties of the cervical spinal ligaments under fast strain-rate deformations, *Acta Biomater* **4**:117−125, 2008.
27. Haut RC, Little RW, A constitutive equation for collagen fibers, *J Biomech* **5**:423−430, 1972.
28. Sauren AAHJ, Hout MC, van Steenhoven AA, van Veldpaus FE, Janssen JD, The mechanical properties of porcine aortic valve tissues, *J Biomech* **16**:327−337, 1983.
29. Kwan MK, Lin TH, Woo SL, On the viscoelastic properties of the anteromedial bundle of the anterior cruciate ligament, *J Biomech* **26**:447−452, 1993.
30. Thornton GM, Oliynyk A, Frank CB, Shrive NG, Ligament creep cannot be predicted from stress relaxation at low stress: A biomechanical study of the rabbit medial collateral ligament, *J Orthop Res* **15**:652−656, 1997.
31. Funk JR, Hall GW, Crandall JR, Pilkey WD, Linear and quasi-linear viscoelastic characterization of ankle ligaments, *J Biomech Eng* **122**:15−22, 2000.
32. Provenzano P, Lakes R, Keenan T, Vanderby R, Nonlinear ligament viscoelasticity, *Ann Biomed Eng* **29**:908−914, 2001.
33. Elliott DM, Robinson PS, Gimbel JA, Sarver JJ, Abboud JA, Iozzo RV, Soslowsky LJ, Effect of altered matrix proteins on quasilinear viscoelastic properties in transgenic mouse tail tendons, *Ann Biomed Eng* **31**:599−605, 2003.
34. Woo SL, Abramowitch SD, Kilger R, Liang R, Biomechanics of knee ligaments: Injury, healing, and repair, *J Biomech* **39**:1−20, 2006.
35. Abramowitch SD, Zhang X, Curran M, Kilger R, A comparison of the quasi-static mechanical and non-linear viscoelastic properties of the human semitendinosus and gracilis tendons, *Clin Biomech* **25**:325−331, 2010.
36. Aalto TJ, Airaksinen O, Harkonen TM, Arokoski JP, Effect of passive stretch on reproducibility of hip range of motion measurements, *Arch Phys Med Rehabil* **86**:549−557, 2005.
37. Boone DC, Azen SP, Normal range of motion of joints in male subjects, *J Bone Joint Surg Am* **61**:756−759, 1979.
38. Greene WB, Heckman JD (eds.), *The Clinical Measurement of Joint Motion*, American Academy of Orthopaedic Surgeons, Rosemont, 1994.
39. Kendall FP, McCreary EK, *Muscles: Testing and Function with Posture and Pain*, Lippincott Williams & Wilkins, Philadelphia, 1993.
40. Roaas A, Andersson GB, Normal range of motion of the hip, knee and ankle joints in male subjects, 30−40 years of age, *Acta Orthop Scand* **53**:205−208, 1982.
41. Roach KE, Miles TP, Normal hip and knee active range of motion: The relationship to age, *Phys Ther* **71**:656−665, 1991.
42. Svenningsen S, Terjesen T, Auflem M, Berg V, Hip motion related to age and sex, *Acta Orthop Scand* **60**:97−100, 1989.
43. Delagi EF, Perotto AO, Iazzetti J, Morrison D, *Anatomical Guide for the Electromyographer: The Limbs and Trunk*, Thomas, Springfield, 1994.
44. Zatsiorsky VM, *Kinetics of Human Motion*, Human Kinetics, Champaign, 2002.
45. De Leva P, Adjustments to Zatsiorsky−Seluyanov's segment inertia parameters, *J Biomech* **29**:1223−1230, 1996.
46. Kirkwood RN, Culham EG, Costigan P, Radiographic and non-invasive determination of the hip joint center location: Effect on hip joint moments, *Clin Biomech* **14**:227−235, 1999.

47. Toms SR, Dakin GJ, Lemons JE, Eberhardt AW, Quasi-linear viscoelastic behavior of the human periodontal ligament, *J Biomech* **35**:1411−1415, 2002.
48. Sarver JJ, Robinson PS, Elliott DM, Methods for quasi-linear viscoelastic modeling of soft tissue: Application to incremental stress-relaxation experiments, *J Biomech Eng* **125**:754−758, 2003.
49. Abramowitch SD, Woo SL, An improved method to analyze the stress relaxation of ligaments following a finite ramp time based on the quasi-linear viscoelastic theory, *J Biomech Eng* **126**:92−97, 2004.
50. Provenzano PP, Heisey D, Hayashi K, Lakes R, Vanderby R, Jr., Subfailure damage in ligament: A structural and cellular evaluation, *J Appl Physiol* **92**:362−371, 2002.
51. Lucas SR, Bass CR, Crandall JR, Kent RW, Shen FH, Salzar RS, Viscoelastic and failure properties of spine ligament collagen fascicles, *Biomech Model Mechanobiol* **8**:487−498, 2009.
52. Johns RJ, Wright J, Relative importance of various tissues in joint stiffness, *J Appl Physiol* **17**:824−828, 1962.
53. Tittel K, *Beschreibende und Funktionelle Anatomie des Menschen*, Urban & Fischer, München, 2003.
54. Sauren AAHJ, Rousseau EPM, A concise sensitivity analysis of the quasi-linear viscoelastic model proposed by Fung, *J Biomech Eng* **105**:92−95, 1983.
55. Winter DA, *Biomechanics and Motor Control Of Human Movement*, Wiley, New York, 1990.